Molecular Biology of the Cell
Vol. 19, 4717–4729, November 2008

Antagonistic Regulation of Cell-Matrix Adhesion by FosB and ΔFosB/Δ2ΔFosB Encoded by Alternatively Spliced Forms of *fosB* Transcripts

Yoshinori N. Ohnishi, Kunihiko Sakumi, Katsuhisa Yamazaki, Yoko H. Ohnishi, Tomofumi Miura, Yohei Tominaga, and Yusaku Nakabeppu

Division of Neurofunctional Genomics, Department of Immunobiology and Neuroscience, Medical Institute of Bioregulation, Kyushu University, Fukuoka 812-8582, Japan

Submitted August 9, 2007; Revised August 8, 2008; Accepted August 20, 2008
Monitoring Editor: William P. Tansey

Among *fos* family genes encoding components of activator protein-1 complex, only the *fosB* gene produces two forms of mature transcripts, namely *fosB* and Δ*fosB* mRNAs, by alternative splicing of an exonic intron. The former encodes full-length FosB. The latter encodes ΔFosB and Δ2ΔFosB by alternative translation initiation, and both of these lack the C-terminal transactivation domain of FosB. We established two mutant mouse embryonic stem (ES) cell lines carrying homozygous *fosB*-null alleles and *fosB*^{d} alleles, the latter exclusively encoding ΔFosB/Δ2ΔFosB. Comparison of their gene expression profiles with that of the wild type revealed that more than 200 genes were up-regulated, whereas 19 genes were down-regulated in a ΔFosB/Δ2ΔFosB-dependent manner. We furthermore found that mRNAs for basement membrane proteins were significantly up-regulated in *fosB*$^{d/d}$ but not *fosB*-null mutant cells, whereas genes involved in the TGF-β1 signaling pathway were up-regulated in both mutants. Cell-matrix adhesion was remarkably augmented in *fosB*$^{d/d}$ ES cells and to some extent in *fosB*-null cells. By analyzing ES cell lines carrying homozygous *fosB*^{FN} alleles, which exclusively encode FosB, we confirmed that FosB negatively regulates cell-matrix adhesion and the TGF-β1 signaling pathway. We thus concluded that FosB and ΔFosB/Δ2ΔFosB use this pathway to antagonistically regulate cell matrix adhesion.

INTRODUCTION

Fos family proteins form heterodimers with Jun family proteins and constitute AP-1 transcription factors. These regulate the expression of various genes, which in turn modulate cell proliferation, differentiation, and cell death (Nakabeppu *et al.,* 1988; Shaulian and Karin, 2001; Miura *et al.,* 2005). Among *fos* family genes, only *fosB* produces two forms of mature transcripts, namely *fosB* and Δ*fosB* mRNAs, by alternative splicing of an exonic intron in exon 4 (see Figure 1A). The former encodes full-length FosB protein, whereas the latter encodes ΔFosB protein (Nakabeppu and Nathans, 1991). The ΔFosB protein is a C-terminal-truncated form of FosB and lacks the C-terminal transactivation domain and the TATA-binding protein (TBP)-binding domain. It has been proposed that FosB dramatically enhances Jun transcription regulation of AP-1–dependent promoters, whereas, based on reporter assays, ΔFosB suppresses this Jun function in a dominant-negative manner (Nakabeppu and Nathans, 1991).

We have reported that ΔFosB has the potential to trigger cell proliferation of quiescent embryonic cell lines or primary neuronal precursor cells and to induce delayed morphological changes or apoptosis dependent on the cell type (Nakabeppu *et al.,* 1993; Nishioka *et al.,* 2002; Tahara *et al.,* 2003; Kurushima *et al.,* 2005), whereas Nestler's group have found that ΔFosB plays an essential role in long-term adaptive changes in the brain associated with diverse conditions in their studies of mice with an inducible-ΔFosB transgene (McClung *et al.,* 2004). Their mice provide a suitable model for the inducible expression of ΔFosB, but the authentic role of this protein remains unclear because the effects of exogenous ΔFosB expression are likely to be modified by endogenous FosB or ΔFosB expression, or vice versa. Furthermore, it has been reported that Δ*fosB* mRNA also produces Δ2ΔFosB protein lacking a N-terminal Fos homology domain (FH) by alternative translation initiation (Sabatakos *et al.,* 2000). To elucidate the authentic function of each protein, it is essential to establish mutants expressing only one of these from an endogenous *fosB* gene.

In the present study, we initially established two mutant embryonic stem (ES) cell lines carrying homozygous *fosB*-null alleles and *fosB*^{d} alleles. The former cells express neither FosB nor ΔFosB/Δ2ΔFosB, and the latter express only ΔFosB and Δ2ΔFosB from artificially manipulated *fosB*^{d} alleles. Both mutant ES cells are devoid of FosB; therefore common phenotypes shared by the two mutants but not by the wild type depict the effects of FosB deficiency, whereas opposite phenotypes in the two are considered to be due to ΔFosB/Δ2ΔFosB. By comparing the gene expression profiles and cellular functions of these two mutants with the wild-type ES cells, we found that ΔFosB/Δ2ΔFosB positively regulates cell-matrix adhesion. Finally, by establishing ES cell lines carrying homozygous *fosB*^{FN} alleles that exclusively encode FosB, we confirmed that FosB negatively regulates cell-matrix adhesion.

MATERIALS AND METHODS

Targeting Vectors

A 19-kb genomic fragment containing an entire sequence of the *fosB* gene was isolated from a 129/Sv mouse genomic library (Stratagene, La Jolla, CA) to

This article was published online ahead of print in *MBC in Press* (http://www.molbiolcell.org/cgi/doi/10.1091/mbc.E07–08–0768) on August 27, 2008.

Address correspondence to: Yusaku Nakabeppu (yusaku@bioreg.kyushu-u.ac.jp).

© 2008 by The American Society for Cell Biology

generate two types of *fosB*-targeting constructs. In the pTV*fosB*^{dN} vector, a pol II-*neo*-poly(A) cassette flanked by two *loxP* sites was placed at the ScaI site of intron 3 in opposite orientation to the *fosB* gene. To generate a mutant *fosB* allele (*fosB*^{dN}), which exclusively encodes ΔFosB protein, the two codons (GTG, AGA) after the last codon (GAG) for ΔFosB (Glu237) were changed. These also function as an alternative splicing donor site for the exonic intron in exon 4 of the *fosB* gene to produce ΔFosB mRNA and were replaced by two tandem stop codons (TAG, TGA) by PCR-mediated site-directed mutagenesis using a Mega-primer protocol (see Figure 1B; Sarkar and Sommer, 1990). The initial PCR was performed with FB8 and FB9, a set of primers with designed mutations, and the BglII fragment (4432 base pairs) containing exon 3 and exon 4 of the *fosB* gene was used as a template using high-fidelity Pyrobest DNA polymerase (Takara Bio, Tokyo, Japan). The second PCR was performed with primer FB10 and with the resulting PCR product as a Mega-primer and using the same template as with the first PCR using zTaq DNA polymerase (Takara Bio).

Next, the AatII-SgrAI fragment, excised from the PCR product, was reciprocally exchanged with the corresponding region surrounding exon 4 of the targeting vector. In the pTV-*fosB*^{GN} vector, a *fosB* gene fragment extending from the NcoI site of exon 2 to the PstI site of exon 3 was replaced with d2EGFP cDNA in-frame and followed the inverted *neo* cassette flanked by two *loxP* sites. The d2EGFP cDNA used was excised from the d2EGFP-N1 vector, which encodes a destabilized variant of EGFP (Clontech, Palo Alto, CA). In each construct, the modified mouse genomic fragment was flanked by herpes simplex virus (HSV)-1 and HSV-2 *thymidine kinase* (*TK*) cassettes (Rancourt *et al.*, 1995). In the pTV*fosB*^{FN} vector, we substituted three bases (GAGGTGAGA→GAAGTTCGA) in the alternative splicing donor site and two bases (AGTGAA→TCTGAA) in the splice acceptor site by PCR-mediated site-directed mutagenesis in order to avoid alternative splicing, which results in the production of ΔFosB (see Figure 7A). The initial PCR was performed with a primer set consisting of FB12 and FB15, the latter carrying designed mutations in the splice acceptor site, and the BglII fragment containing exon 3 and exon 4 of the *fosB* gene was used as a template. The second PCR was performed with primer FB16 carrying designed mutations in the splice donor site and with the resulting PCR product as a Mega-primer, using the same template. The third PCR was performed with primer FB10 and the resulting PCR product as a Mega-primer, using the same template as with the first PCR. Finally, the AatII-SgrAI fragment, excised from the third PCR product, was reciprocally exchanged with the corresponding region surrounding exon 4 of the targeting vector. PCR primers used for construction of targeting vectors are listed in Table 1.

Table 1. Primers used in the present study

FB1	5′-ACGGTCACCGCAATCACAAC-3′
FB2	5′-TAGCTGGTTCCTGGCATGT-3′
FB3	5′-AGAGCGAGGGAAGCGTCTACCTA-3′
FB4	5′-CTCGTTTAGGACACAGGCACAGT-3′
FB5	5′-GACGCTTCGACAGGATTGG-3′
FB6	5′-GGGGTGTTCTGCTGGTAGT-3′
FB7	5′-TGCAAGATCCCCTACGAAGAG-3′
FB8	5′-GAGTCGCCTTGTTCCTTGCGGG-TTTG-3′
FB9	5′-GCCGAGTAGTGAGATTTGCCAGGG-TCAACA-3′
FB10	5′-GCTTGGAGTTCTTGCCTATC-3′
FB11	5′-CAAGAAGGGAGGGCGAGTT-3′
FB12	5′-GCAGGTGGTCAGACAGAAGAGT-3′
FB13	5′-CAATGCCCCCTTCTGCCCTTTA-3′
FB14	5′-TGCTACTTGTGCCTCGGTTTCC-3′
FB15	5′-ACTCTGAAGTTCAAGTCCTCGG-CGAC-3′
FB16	5′-GCCGAAGTTCGAGATTTGCCAGGG-TCAACA-3′
c-fos (Forward)	5′-GTTTCAACGCCGACTACGA-3′
c-fos (Reverse)	5′-CACCGTGGGGATAAAGTTG-3′
fra-1 (Forward)	5′-TGCAGAAGCAGAAGGAACG-3′
fra-1 (Reverse)	5′-TGCTGCTGCTACTCTTTCG-3′
fra-2 (Forward)	5′-ATCCCGGGAACTTTGACAC-3′
fra-2 (Reverse)	5′-TTCTGCAGCCCAGACTTCT-3′
Lama1 (Forward)	5′-GTACATTCGCCTTCGTCTG-3′
Lama1 (Reverse)	5′-GCATGGATCCTCATTCAGG-3′
Lamb1–1 (Forward)	5′-TCTGGTGGCAATCGGAAAAT-GGTG-3′
Lamb1–1 (Reverse)	5′-GTTCAGGCCTTTGGTGTTGTG-TCT-3′
Lamc1 (Forward)	5′-GGTGACAAAGCCGTAGAG-3′
Lamc1 (Reverse)	5′-ACTGCGTCCCTTCTTAGC-3′
Col4a1 (Forward)	5′-CATTCAGATTCCGCAGTGC-3′
Col4a1 (Reverse)	5′-ATCAGGAGCGCCATTTGGT-3′
Col4a2 (Forward)	5′-CAGGATTCCAAGGTGCTCA-3′
Col4a2 (Reverse)	5′-CCTTGGTCGCCTTTCTTTC-3′
Gata6 (Forward)	5′-ACCGGTCATTACCTGTGCA-3′
Gata6 (Reverse)	5′-TTGGCGTTTTCTCCCACTG-3′
Ilk (Forward)	5′-GAATGAGCACGGCAATGT-3′
Ilk (Reverse)	5′-GCCATGTCCAAAGCAAAC-3′
Akt1 (Forward)	5′-CGTGTGGCAGGATGTGTAT-3′
Akt1 (Reverse)	5′-GGTCGCGTCAGTCCTTAAT-3′
Thbs1 (Forward)	5′-CGATGGAGATGGAATCCTC-3′
Thbs1 (Reverse)	5′-CCATCACCATCAGAGTCCT-3′
Gapdh (Forward)	5′-TGGTATTCAAGAGAGTAGGGA-3′
Gapdh (Reverse)	5′-CTGCCATTTGCAGTGGCAAAG-3′
Tgfb1 (Forward)	5′-ACAGGGCTTTCGATTCAGC-3′
Tgfb1 (Reverse)	5′-GCGCACAATCATGTTGGAC-3′
Tgfb1i1 (Forward)	5′-GTGGCTTCTGTAACCAACC-3′
Tgfb1i1 (Reverse)	5′-GATCTCTGATCCCAAGAGG-3′
Tgfb1i1 (Forward) for qRT-PCR	5′-AAGGCAGTCTGGACACCAT-3′
Tgfb1i1 (Reverse) for qRT-PCR	5′-ACAACCGCTGCAAAGGAAG-3′
Gapdh (Forward) for qRT-PCR	5′-AAATGGTGAAGGTCGGTGTG-3′
Gapdh (Reverse) for qRT-PCR	5′-TGAAGGGGTCGTTGATGG-3′
CMV promoter (Forward)	5′-AATGGGGCGGAGTTGTTACGA-3′
CMV promoter (Reverse)	5′-CGGGGTCATTAGTTCATAGCC-3′
CRE recombinase (Forward)	5′-TTACGTATATCCTGGCAGCG-3′
CRE recombinase (Reverse)	5′-TTCGCAAGAACCTGATGGAC-3′

Cell Culture

CCE cells, a mouse ES cell line derived from a 129SvEv mouse, were maintained as previously described (Robertson, 1987; Ide *et al.*, 2003). To obtain quiescent ES cells, cells subcultured twice without feeder cells were maintained in ES medium supplemented with 0.5% FBS for 3 d without changing the medium. To obtain serum-stimulated ES cells, the quiescent ES cells were stimulated by exchanging the medium for fresh ES medium supplemented with 20% FBS.

Generation of fosB Mutant ES Cell Lines

CCE cells were electroporated with the linearized targeting vector DNA, and colonies doubly resistant to G418 and gancyclovir were selected as described (Robertson, 1987; Ide *et al.*, 2003). Correctly targeted clones were identified by Southern blotting and genomic PCR analyses. The introduced mutations were confirmed by direct sequencing of each genomic PCR product containing the entire exonic intron in *fosB* exon 4 amplified with a set of primers, FB7 and FB12, using FB11 as the sequencing primer. Twenty clones of *fosB*$^{+/dN}$, 4 clones of *fosB*$^{+/GN}$, and 3 clones of *fosB*$^{+/FN}$ heterozygous ES mutants were independently identified. Subsequently, each heterozygous ES mutant was cultured in the presence of increasing concentrations of G418 (1.2–1.5 mg/ml) for 9 d and then 1.0 mg/ml G418 for 5 d in order to isolate ES cells carrying the two mutant alleles with the *neo* cassette generated by homologous recombination of the wild-type and mutant alleles. Resistant colonies were picked up and homozygotes for each mutant allele were identified by Southern blotting and direct sequencing of their genomic PCR products. Five clones of *fosB*$^{dN/dN}$, 13 clones of *fosB*$^{GN/GN}$, and 3 clones of *fosB*$^{FN/FN}$ were independently established. To excise the *neo* cassette flanked by the *loxP* sites in the targeted allele, a Cre expression vector, pBS185 (Invitrogen, Carlsbad, CA), was introduced into *fosB*$^{dN/dN}$ or *fosB*$^{+/dN}$ ES cells by electroporation. Excision of the *neo* cassette in each colony formed in the absence of G418 was confirmed by Southern blotting and genomic PCR (see Figure 2, A and E). Thus, the generated allele was designated the *fosB*^{d} allele, and 9 *fosB*$^{d/d}$ and 10 *fosB*$^{+/d}$ clones were independently isolated. No genomic PCR product was amplified from any of the established homozygous clones using two-primer sets for part of the Cre coding sequence and the CMV promoter region in pBS185.

Western Blot Analysis

Nuclei were isolated from ES cells maintained in the absence of feeder cells using NP-40 lysis buffer (10 mM Tris-HCl, pH 7.4, 10 mM KCl, 1.5 mM $MgCl_2$, 0.5% NP-40, 0.1% DNase, 0.05% RNase, and protease/phosphatase inhibitors). Each sample was subjected to 12.5% SDS-PAGE and Western blot

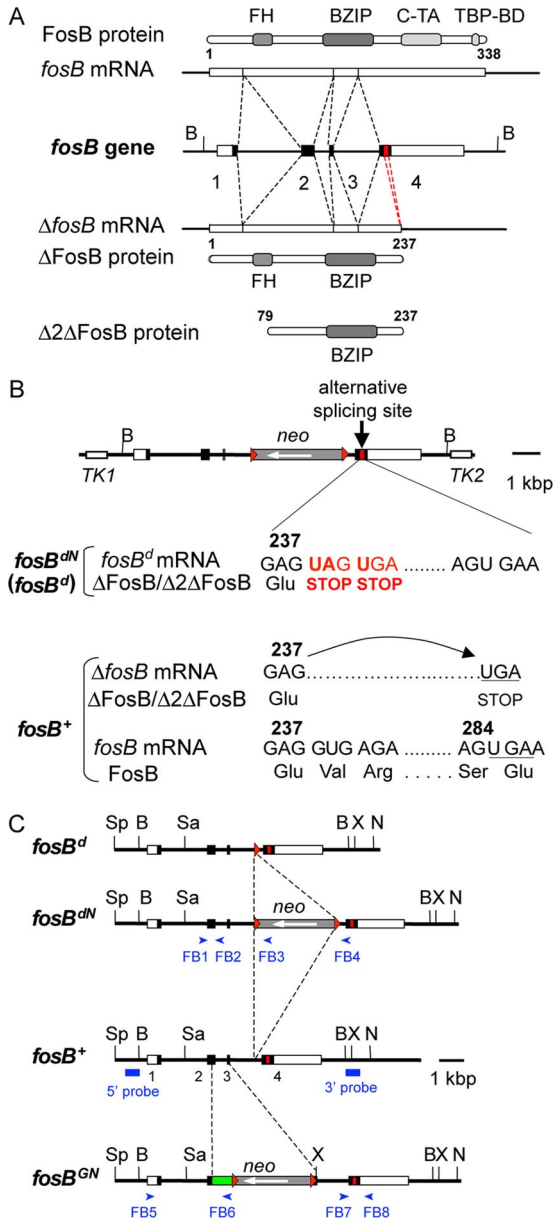

Figure 1. Strategy for generation of mutant *fosB* alleles by gene targeting. (A) Genomic organization of the mouse *fosB* gene, its transcripts (*fosB* and Δ*fosB* mRNAs) and translation products (FosB, ΔFosB, and Δ2ΔFosB proteins) are shown. FH, N-terminal Fos homology domain; BZIP, basic region and leucine zipper; C-TA, C-terminal transactivation domain; TBP-BD, TBP-binding domain. Each pair of dotted lines indicates the splicing of each intron and a red box indicates an exonic intron in exon 4, which is alternatively spliced out (red dotted lines). (B) Strategy for generation of a $fosB^d$ allele that encodes only ΔFosB/Δ2ΔFosB. The targeting vector, pTV-$fosB^{dN}$, carries all exons and introns of the *fosB* gene flanked by two HSV-*TK* genes (*TK1, TK2*) at BamHI sites, labeled B. Two tandem stop codons (red letters) were introduced by three base substitutions (bold letters) at the alternative splicing site in exon 4. Gray box, *neo* cassette; white arrow, direction of the *neo* gene; red triangle, *loxP* site. Sequences of a transcript ($fosB^d$ mRNA) from the $fosB^d$ or $fosB^{dN}$ allele or from the wild-type ($fosB^+$) allele, and the corresponding amino acid residues are shown. The arc with an arrowhead indicates the alternative splicing of the exonic intron (red box). (C) Structures of mutant *fosB* alleles. The $fosB^d$ allele was generated by transient expression of Cre recombinase in cells carrying homozygous $fosB^{dN}$ alleles. In the $fosB^{GN}$ allele, parts of exon 2 and exon 3 with intron 2 were replaced with d2EGFP and the *neo* cassette with two loxP sites. Blue arrowheads, primers used for RT-PCR, genomic PCR, and sequencing of the products; blue bars, probes for Southern blotting, green box, d2EGFP cDNA; Sp, SpeI; B, BamHI; Sa, SacI; X, XhoI; N, NotI.

analysis as previously described (Nakabeppu *et al.*, 1993; Tsuchimoto *et al.*, 2001). Anti-FosB(N) was raised against amino acids 79–130 of the N-terminus of FosB or ΔFosB, whereas anti-FosB(C) was raised against amino acids 245–315 of the C-terminus of FosB (Nakabeppu and Nathans, 1991). Anti-c-Fos (sc-52) was obtained from Santa Cruz Biotechnology (Santa Cruz, CA).

cDNA Microarray Analysis

Total RNA was purified from ES cells grown in the absence of feeder cells using ISOGEN (Nippon Gene, Tokyo, Japan), according to the manufacturer's instructions. For DNA microarray experiments, total RNA (10 μg) was labeled using an Agilent Linear Amplification/Labeling kit (Agilent Technologies, Wilmington, DE) according to the manufacturer's instructions. A mixture was made of 1 μg of each Cy3-labeled wild-type and Cy5-labeled mutant cDNA or each Cy3-labeled mutant and Cy5-labeled wild-type cDNA, and these cDNAs were then hybridized to Agilent Mouse cDNA Microarrays (G4104A, design file number: 000522R000679, Agilent Technologies) with 8500 unique clones from the Incyte mouse UniGene 1 clone set, according to the manufacturer's hybridization protocol. After washing, the microarray slides were analyzed with an Agilent G2565AA microarray scanner system. These experiments were carried out in duplicate using exchanged dye-labeled cDNA probes (as in Cy3 and Cy5 dye-swapping experiments). Data analysis was performed using Agilent Feature Extraction software (Ver. A.6.1.1) and Excel 2002 (Microsoft, Redmond, WA). Genes whose expression levels in mutant ES cells were altered significantly in comparison to those in wild-type ES cells with a p value < 0.01 were retrieved.

Cell-Matrix Adhesion Assay

ES cells maintained in the absence of feeder cells were prepared for the cell-matrix adhesion assay as 1) exponentially growing, 2) quiescent, or 3) serum-stimulated for 4 h, as described above. Each preparation of ES cells was plated at various concentrations (0.5×10^5, 1.0×10^5, 2.0×10^5 and 4.0×10^5 cells per well [1.9 cm^2]) on five types of coated and noncoated 24-well plates in ES medium supplemented with 20% FBS and incubated for 4 h. Surfaces of the 24-well plates were coated with five different matrices consisting of 0.1% gelatin, 10 μg/ml collagen type I, 10 μg/ml collagen type IV, 10 μg/ml fibronectin, and 10 μg/ml laminin (Sigma-Aldrich, St. Louis, MO). After fixation with 25% glutaraldehyde, attached cells were stained with 0.3% crystal violet, and the dye was extracted in 50% ethanol to measure absorbance at 595 nm, which provides a reading that is proportional to the number of cells attached. A one-way ANOVA with Dunnett's post hoc test was performed to assess the number of cells that attached at a concentration of 2.0×10^5 cells per well, using KaleidaGraph (Synergy Software, Reading, PA).

Southern Blot Analysis

Southern blot analysis was carried out as described (Ide *et al.*, 2003; Xu *et al.*, 2003). Isolated genomic DNA was digested with XhoI and SpeI, or with NotI and SacI, separated in 0.8% agarose gel, and transferred to nylon membranes (GE Healthcare Bio-Science, Piscataway, NJ) by capillary blotting. The membrane was hybridized with a random-primed ^{32}P-labeled probe using standard methods.

RT-PCR Analysis

Total RNA was prepared from cultured cells using ISOGEN. First-strand cDNA was synthesized using a first-strand cDNA synthesis kit (GE Healthcare Bio-Sciences) according to the manufacturer's instructions. Subsequently, PCR was performed with the primers listed in Table 1. For quantitative real-time RT-PCR for *Tgfb1i1* mRNA, reactions in triplicate were performed using an Applied Biosystems 7500 Real-Time PCR System with SYBR Green Master Mix (Applied Biosystems, Foster City, CA) and the primers listed in Table 1. The expression level was determined by normalization with *Gapdh* mRNA, and a relative level of *Tgfb1i1* mRNA in each cell line to that in the wild-type ES cells was calculated.

RESULTS

Establishment of fosB Mutant ES Cell Lines

To create an altered allele of *fosB*, namely $fosB^d$, which can produce only the ΔFosB and Δ2ΔFosB, but not the FosB protein, we introduced two tandem stop codons into the *fosB* gene after the last codon for Glu237 of ΔFosB (Figure 1B). These base substitutions also disrupt the splicing donor sequence, and it was therefore expected that the $fosB^d$ allele

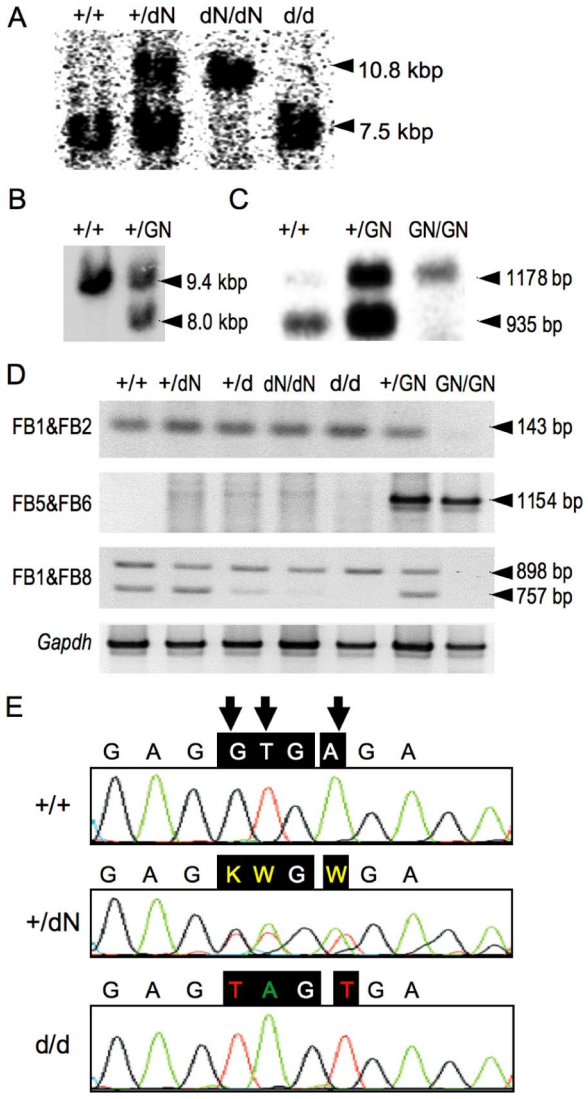

Figure 2. Establishment of ES cell lines carrying mutant *fosB* alleles by gene targeting. (A) Southern blot analysis of $fosB^{dN}$ and $fosB^{d}$ alleles. A single 7.5-kbp band was detected in the wild type ($fosB^{+/+}$), whereas a 10.8-kbp band was detected as a fragment derived from the $fosB^{dN}$ allele in the $fosB^{+/dN}$ heterozygote. In the $fosB^{dN/dN}$ homozygote, only the 10.8-kbp band was detected. In the $fosB^{d/d}$ homozygote, a single 7.5-kbp band was detected in which the 3.3-kbp *neo* cassette was excised by Cre recombinase. (B) Southern blot analysis of the $fosB^{GN}$ allele. In the wild type, a 9.4-kbp band was detected, whereas an additional 8.0-kbp band was detected as a fragment derived from the $fosB^{GN}$ allele in the $fosB^{+/GN}$ heterozygote. (C) Genomic PCR analysis of the $fosB^{GN}$ allele. From the wild-type allele, a 935-base pair band was amplified by FB1 and FB4, whereas a 1178-base pair band was amplified from the $fosB^{GN}$ allele with FB1 and FB3. (D) RT-PCR analysis of the mutant *fosB* transcripts. Total RNA was prepared from ES cells stimulated for 45 min with 20% serum. With the primers FB1 and FB2 (top panel), a 143-base pair fragment was expected to be amplified from *fosB* transcripts from wild-type, $fosB^{dN}$, and $fosB^{d}$ alleles but not from the $fosB^{GN}$ allele. With the primers FB5 and FB6 (the second panel), a 1154-base pair fragment was expected to be amplified from FosB(N)-d2EGFP fusion mRNA transcribed from the $fosB^{GN}$ allele. With the primers FB1 and FB8 (third panel), an 898-base pair fragment from FosB mRNA and a 757-base pair fragment from ΔFosB mRNA were expected to be amplified. *Gapdh* mRNA was amplified as an internal control (bottom panel). (E) Sequencing analysis of genomic PCR products. Genomic DNA prepared from wild-type and $fosB^{+/dN}$ and $fosB^{d/d}$ ES cells was subjected to PCR amplification with primers FB7 and FB8, and base substitutions (arrows) introduced into the mutant alleles were confirmed by direct sequencing. In the sequence for +/dN, K represents two peaks for guanine and thymine, whereas W represents two peaks for adenine and thymine.

would produce only the longer form of the *fosB* transcript, designated $fosB^{d}$ mRNA. In pTV$fosB^{dN}$, a targeting vector shown in Figure 1B, the altered *fosB* allele ($fosB^{dN}$) contains a *neo* cassette for positive selection, which is flanked by *loxP* sites. The *neo* cassette can be excised by Cre recombinase, thereby generating the $fosB^{d}$ allele. We also constructed pTV-$fosB^{GN}$, a targeting vector in which d2EGFP cDNA encoding a destabilized variant of enhanced green fluorescent protein (EGFP) was placed in exon 2 in frame, and the remainder of exon 2 and the entire exon 3 were replaced by a *neo* cassette flanked by *loxP* sites.

By means of homologous recombination and transient expression of Cre recombinase, we successfully established $fosB^{d/d}$ and $fosB^{GN/GN}$ ES cell lines, respectively (Figure 2, A–C). The $fosB^{d}$ allele produced only the longer transcript that is expected to encode only ΔFosB (Figure 2D, dN/dN and d/d), whereas the $fosB^{GN}$ allele produced the *fosB*:*d2EGFP* fusion transcript (Figure 2D, +/GN, GN/GN), which may encode a nonfunctional FosB:d2EGFP fusion protein. In $fosB^{+/dN}$ and $fosB^{d/d}$ mutant ES cells, we confirmed the base substitutions introduced at the alternative splicing site by direct sequencing of their genomic PCR fragments (Figure 2E).

RT-PCR analysis revealed that low but substantial levels of *fosB* transcripts were expressed in quiescent wild-type and $fosB^{d/d}$ and $fosB^{GN/GN}$ ES cells (Figure 3A, quiescent). After serum stimulation, large amounts of the two types of *fosB* transcripts, namely *fosB* and Δ*fosB* mRNAs, respectively, which encode FosB and ΔFosB/Δ2ΔFosB, were transiently induced in wild-type cells (Figure 3A, +/+), whereas only the longer form of the transcripts, namely $fosB^{d}$ mRNA, which is expected to encode ΔFosB and Δ2ΔFosB, was transiently induced in $fosB^{d/d}$ cells (Figure 3A, d/d). In serum-stimulated $fosB^{GN/GN}$ ES cells, two types of *fosB* transcripts were detected, but the level of the shorter form was much lower than that of the longer form (Figure 3A, GN/GN), suggesting that replacement of exons 2–3 with an EGFP-*neo* cassette may alter the efficiency of the alternative splicing. After serum stimulation, levels of c-*fos*, *fra-1*, and *fra-2* mRNAs were also transiently increased in $fosB^{d/d}$ and $fosB^{GN/GN}$ ES cells as they were in the wild type (Figure 3A). Among the three cell lines, the highest levels of *fra-2* mRNA were observed in $fosB^{d/d}$ cells, with or without serum stimulation. Furthermore, it was noteworthy that the levels of *c-fos* and *fosB* transcripts in the quiescent $fosB^{d/d}$ and to a lesser extent $fosB^{GN/GN}$ cells or in these cells 4 h after serum stimulation, were apparently higher than in the wild type, probably because of their lack of the functional FosB protein, which can suppress transcription of *c-fos* and *fosB* genes (Nakabeppu and Nathans, 1991; Lazo *et al.*, 1992).

To compare expression of FosB and ΔFosB/Δ2ΔFosB proteins in each type of mutant ES cell, Western blotting analyses were performed as shown in Figure 3, B–D. Expression of *fosB* gene products was barely detectable in quiescent ES cells, irrespective of the *fosB* genotype. In the serum-stimulated wild-type, 43- and 32/36-kDa polypeptides were detected by Western blotting with anti-FosB(N), which reacts with both FosB and ΔFosB, and the 43-kDa polypeptide was also detected by anti-FosB(C), which reacts only with FosB (Nakabeppu and Nathans, 1991). In the $fosB^{d/d}$ cells, how-

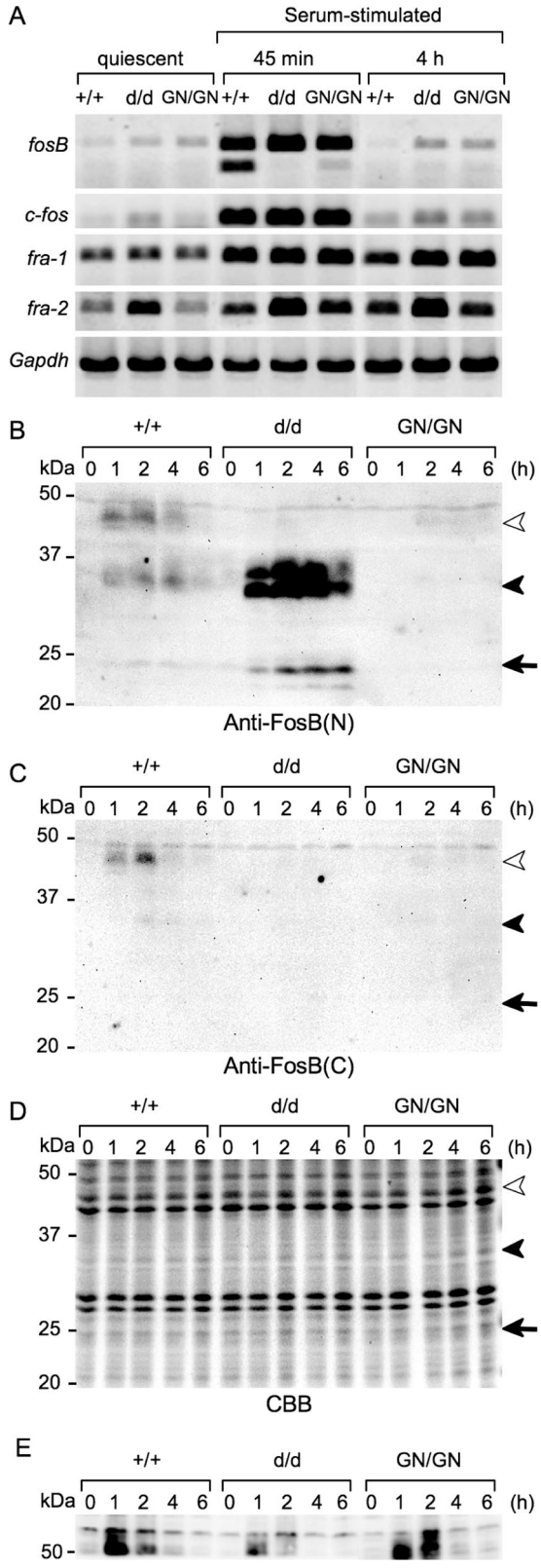

Figure 3. Characterization of ES cell lines carrying mutant *fosB* alleles. (A) RT-PCR analysis of *fos* family mRNAs after serum stimulation. *fosB* cDNA was amplified with primers FB7 and FB8. (B) Western blotting with anti-FosB(N). Nuclear extracts (100 μg per lane) prepared from ES cells at given times after serum stimulation of quiescent cells (0 h) were subjected to Western blotting with anti-FosB(N), which reacts with both FosB and ΔFosB. (C) Western blotting with anti-FosB(C). A sister blot prepared as shown in B was probed with anti-FosB(C), which reacts with only with FosB. (D) A sister gel stained with Coomassie brilliant blue (CBB). In B–D, open arrowheads indicate p43, the closed arrowhead indicates p32/36, and the arrow indicates p24, respectively. (E) Western blotting with anti-c-Fos. A sister blot prepared as shown in A was probed with anti-c-Fos.

ever, serum stimulation induced a significantly increased expression of the 32/36-kDa polypeptide, namely ΔFosB, whose peak levels were 10 times as high as those of the wild type. There were no detectable polypeptides in the serum-stimulated *fosB*$^{GN/GN}$ cells using either type of anti-FosB, and these cells were therefore designated *fosB*-null ES cells. It was apparent that serum-stimulated *fosB*$^{d/d}$ cells express a 24-kDa polypeptide that was recognized only by anti-FosB(N), and its level was higher than that in the wild type, indicating that this polypeptide is Δ2ΔFosB produced by alternative translation initiation of Δ*fosB* mRNA (Sabatakos *et al.*, 2000). We further found that the expression level of c-Fos protein was apparently down-regulated in serum-stimulated *fosB*$^{d/d}$ ES cells only (Figure 3E) and that similar levels of Fra-1 and Fra-2 proteins were induced in all three ES cells after serum stimulation (data not shown).

Altered Gene Expression Profiles in fosB Mutant ES Cells

Despite the altered expression of *fosB* gene products, *fosB*$^{d/d}$, and *fosB*-null and wild-type ES cells exhibited essentially the same growth rate under normal growth conditions and efficiently differentiated into a neuronal lineage in the presence of retinoic acids. These data are presented as Supplemental Figure S1. To expand our understanding of the biological significance of FosB and ΔFosB/Δ2ΔFosB, we next compared the gene expression profile of each mutant with that of wild-type ES cells using total RNA prepared from cells 4 h after serum stimulation (Figure 4A) and obtained reliable data on 5290 of 8500 unique probes. As shown in Figure 4, B and C, expression of 267 genes (5.05%) was significantly altered in *fosB*$^{d/d}$ cells, whereas that of only 44 genes (0.83%) was affected in *fosB*-null cells, compared with the wild type. Expression of 203 genes was significantly up-regulated in the *fosB*$^{d/d}$ cells, with no remarkable change noted in the *fosB*-null cells (Figure 4D).

Among the genes up-regulated in *fosB*$^{d/d}$ ES cells, more than a quarter encode cell-adhesion–related proteins (Table 2). In particular, genes for laminin α1 (*Lama1*) and Collagen type IV α1 (*Col4a1*), which are major components of the basement membrane in embryonic tissue (Ekblom *et al.*, 2003), were the most significantly up-regulated in *fosB*$^{d/d}$ cells. Three additional genes for Laminin B1 (*Lamb1-1*), γ1 (*Lamc1*) and Collagen type IV α2 (*Col4a2*), proteins comprising the basement membrane, were likely up-regulated in *fosB*$^{d/d}$ cells (Table 3). As shown in Figure 5A, RT-PCR analyses confirmed that expression of *Lama1, Lamb1-1, Lamc1, Col4a,* and *Col4a2* genes was up-regulated in serum-stimulated *fosB*$^{d/d}$ ES cells, and to a much lesser extent in *fosB*-null cells, in comparison to the wild type.

Moreover, we found that expression levels of these five genes in quiescent *fosB*$^{d/d}$ cells were also higher than in the wild type, and serum stimulation did not increase their expression. In the wild-type cells, serum stimulation decreased their expression levels except that of *Lama1* (Figure 5A). On the other hand, genes for GATA6 (*Gata6*), thrombospondin 1 (*Thbs1*), and Akt 1 (*Akt1*) were serum-inducible in the three lines, and their expression levels in *fosB*$^{d/d}$ ES cells were much higher than in *fosB*-null and wild-type cells,

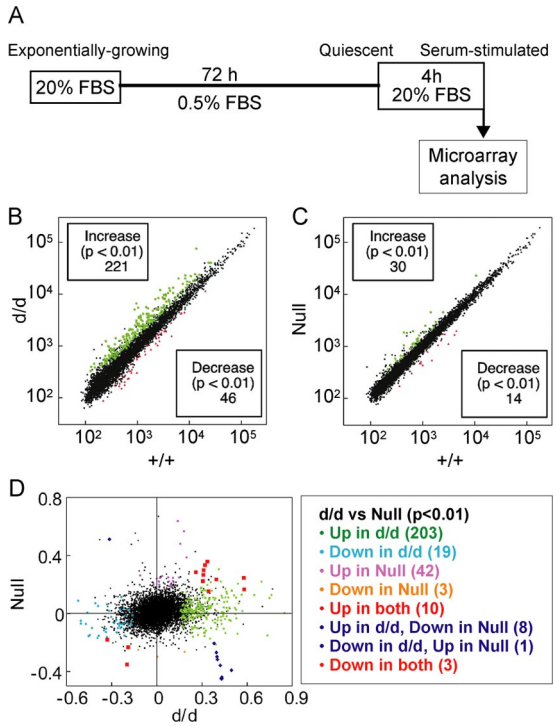

Figure 4. Comparison of gene expression profiles among *fosB* mutant and wild-type ES cells. (A) Experimental schedules. (B) Comparison of gene expression profiles between *fosB*$^{d/d}$ and wild-type ES cells. The average intensity of 5290 processed probes, excluding those with outlier signals and signals lower than the threshold, was plotted as a scatter diagram. Significantly up-regulated genes are shown in green, whereas down-regulated genes are shown in red ($p < 0.01$). (C) Comparison of gene expression profiles of *fosB*-null and wild-type ES cells. Data are shown as in B. (D) Comparison of gene expression profiles of *fosB*$^{d/d}$ and *fosB*-null ES cells on a logarithmic scale. Data were transformed from B and C for comparison with the wild type.

Table 2. Functional classification of genes whose expression was significantly altered in *fosB*$^{d/d}$ *and fosB*-null ES cells in comparison to the wild type, at 4 h after serum stimulation

	No. in *fosB*$^{d/d}$		No. in *fosB*-null	
Category of genes	Up	Down	Up	Down
Cell-adhesion–related proteins	57	2	8	2
Transcription factors and DNA-binding proteins	27	4	4	1
Intracellular signal transduction modulators and effectors	23	1	4	0
Metabolic-enzyme–related proteins	15	5	2	2
Glucolipid metabolism	14	1	1	0
Proteolytic degradation-related proteins	9	1	2	2
Growth and developmental proteins	9	3	3	2
Stress response proteins	8	1	0	1
Calcium-binding proteins	7	1	0	0
Blood coagulation proteins	5	0	1	1
Apoptosis-related proteins	4	0	0	0
Cell cycle regulators	1	1	1	0
Highly expressed at embryonic stage	12	14	3	1
Highly expressed in immune system	4	5	0	1
Highly expressed in mammary gland	3	1	0	1
Highly expressed in skin	2	0	1	0
Highly expressed in alimentary tract	1	3	0	0
Others	20	3	0	0
Total	221	46	30	14

even in quiescence (Figure 5A). These results suggest that the expression level of ΔFosB/Δ2ΔFosB in quiescent *fosB*$^{d/d}$ ES cells must also be higher than in the quiescent wild type, as expected from the data shown in Figure 3A. With a large quantity of nuclear extract (200 μg protein), small but significant amounts of ΔFosB and Δ2ΔFosB were detected not only in the quiescent but also in the exponentially growing *fosB*$^{d/d}$ cells as well (Figure 5B). In contrast, neither wild-type nor *fosB*-null cells exhibited a detectable expression of FosB or ΔFosB/Δ2ΔFosB under these conditions. Therefore, up-regulation of mRNAs for the three types of Laminin-1 and two types of Collagen (IV), but not for GATA6 or Akt 1, had occurred in the exponentially growing *fosB*$^{d/d}$ ES cells (Figure 5C), and this was likely due to the increased level of ΔFosB/Δ2ΔFosB. However, it is noteworthy that under conditions of exponential growth, expression levels of *Lama1*, *Lamb1-1*, *Lamc1*, *Col4a*, *Col4a2*, and *Gata6* genes in wild-type cells were slightly higher than those in *fosB*-null cells, whereas the lowest expression of the *Thbs-1* gene was observed in the wild-type cells (Figure 5C), suggesting that FosB or ΔFosB/Δ2ΔFosB may be expressed in the exponentially growing wild-type cells, thus contributing to their gene expression regulation.

Increased Cell-Matrix Adhesion in fosB$^{d/d}$ *and fosB-null ES Cells*

As shown in Table 3, more than 10 genes encoding proteins involved in basement membrane regulation, such as Integrin-linked kinase (*Ilk*), Nidogen 1 (*Nid1*), Procollagen prolyl 4-hydroxylase α1 and α2 (*P4ha1*, *P4ha2*), Procollagen-lysine, 2-oxoglutarate 5-dioxygenase 1 and 2 (*Plod1*, *Plod2*), and *Thsb1*, were up-regulated in *fosB*$^{d/d}$ ES cells, as were those for major basement membrane components (Supplementary Figure S2). Thus, we examined whether *fosB*$^{d/d}$ ES cells undergo any alteration in cell-matrix adhesion (Figure 6). Exponentially growing *fosB*$^{d/d}$ cells exhibited significantly higher adhesion to uncoated plates or to plates coated with gelatin, collagen type I or IV, laminin, and fibronectin, compared with exponentially growing wild-type cells, whereas *fosB*-null cells exhibited essentially the same adhesive behavior as that of wild-type cells (Figure 6, A–F). Quiescent wild-type cells were found to have dramatically lost their adhesion to plates coated with or without collagen type I, IV or gelatin, and to have moderately lost adhesion to those coated with laminin or fibronectin. In contrast, quiescent *fosB*$^{d/d}$ cells sustained efficient adhesion under any condition, compared with the exponentially growing cells. Interestingly, quiescent *fosB*-null cells exhibited essentially the same high levels of adhesion to laminin and fibronectin as did *fosB*$^{d/d}$ cells, but only an intermediate adhesion to other coating materials or to uncoated plates (Figure 6, G–L). Four hours after serum stimulation of the quiescent cells showed increase in their adhesion to all matrices. Among these,

Table 3. Significantly altered genes related to basement membrane genes on cDNA microarray

Gene symbol[a]	Accession number	Fold change: Cy3 d/d / Cy5 +/+	Fold change: Cy5 d/d / Cy3 +/+	Fold change: Cy3 Null / Cy5 +/+	Fold change: Cy5 Null / Cy3 +/+
Up-regulated in *fosB*$^{d/d}$ ES cells (potential ΔFosB targets)					
Lama1	AA123168	4.40*	4.50*	1.45*	1.22
Lamb1–1	AI551931	6.67*	Outlier	2.17*	Outlier
Lamc1	AA445786	Outlier	3.00*	1.46*	0.86
Col4a1	AA760135	4.93*	6.33*	1.12	1.42*
Col4a2	W53787	4.51*	Outlier	0.87	1.48*
Gata6	AA536899	3.85*	2.92*	1.20	0.64*
Ilk	AA624474	2.34*	1.56*	1.41*	0.92
Akt 1	AA415535	1.61*	1.81*	0.72	0.74
Nid1	AA606605	2.14*	3.61*	1.08	1.87*
P4ha1	AA518751	3.15*	3.60*	1.03	1.09
Plod1	AA681596	3.58*	2.15*	1.41	1.17
Plod2	AI549660	2.48*	3.09*	0.88	1.13
Klf6	AA895718	1.95*	1.51*	0.63*	1.37
Cited1	AA709508	3.18*	2.10*	0.48*	0.40*
Runx1	AA245642	3.25*	2.73*	1.79*	0.79
Elf3	AA822889	2.07*	1.66*	0.78	1.17
Cdh1	AA607208	1.41*	1.52*	1.37	1.43*
Up-regulated in both *fosB*$^{d/d}$ and *fosB*-null ES cells (potential FosB targets)					
Thbs1	AI180914	2.64*	1.71*	2.84*	1.71*
Ankrd1	AA792499	2.83*	2.16*	1.87*	1.57*
P4ha2	AA388310	4.08*	3.56*	1.45*	1.48*

[a] Official gene symbol; * $p < 0.01$.

fosB$^{d/d}$ cells exhibited the highest adhesion to uncoated plates or to plates coated with collagen type I and IV, whereas *fosB*-null cells exhibited the highest adhesion to plates coated with gelatin, laminin, and fibronectin (Figure 6, M–R).

We concluded that *fosB*$^{d/d}$, and to a lesser extent *fosB*-null ES cells, exhibited significantly increased adhesion to plates with or without matrix.

Up-Regulation of TGF-β 1 Signaling in fosB$^{d/d}$ *ES Cells*

It has been reported that constitutively active Akt caused an up-regulation of mRNAs for Laminin 1 and Collagen type IV isotypes in ES cells (Li *et al.*, 2001). Although the protein level of Akt was slightly up-regulated in *fosB*$^{d/d}$ ES cells with or without serum stimulation, phosphorylation of Akt (Ser473, Thr 308), which was barely detectable in the quiescent cells, was transiently induced after serum stimulation, as observed in *fosB*-null and wild-type cells. Furthermore, GSK3β, which is a target of Akt and is expressed constitutively, was also transiently phosphorylated after serum stimulation in all three lines (Supplementary Figure S3).

An increased expression of GATA6 in ES cells is also known to induce expression of laminin 1 (Li *et al.*, 2004); however, among the three ES cell lines, the level of *Gata6* mRNA was remarkably decreased in exponentially growing *fosB*$^{d/d}$ cells (Figure 5C). We suggest that the increased expression of mRNAs encoding the basement membrane proteins and related proteins in *fosB*$^{d/d}$ ES cells is dependent on neither the Akt signaling pathway nor transactivation by GATA6.

Thrombospondin 1/TGF-β1 signaling is known to up-regulate the expression of genes encoding basement membrane proteins, thereby increasing cell-matrix adhesion (Lawler, 2002). As shown in Figure 5, A and C, we found that expression levels of *Thbs1* mRNA under quiescent conditions were lower, but that they differed significantly among the three ES cell lines, compared with those in exponentially growing or serum-stimulated cells, and their order (*fosB*$^{d/d}$ > *fosB*-null > wild type) was the same as that of their cell-matrix adhesion under the quiescent conditions (Figure 6, G–L). Because there was no probe for the TGF-β1 gene (*Tgfb1*) in the cDNA microarray used, we examined its expression level by RT-PCR analysis (Figure 5D) and confirmed an increased expression of *Tgfb1* in serum-stimulated *fosB*$^{d/d}$, but not in *fosB*-null ES cells, in comparison to the wild type. Furthermore, expression of TGF-β1–induced transcript 1 (*Tgfb1i1*) was increased in *fosB*$^{d/d}$ cells and to a lesser extent in *fosB*-null cells, compared with the wild type (Figure 5D). Again, we found that expression levels of *Tgfb1 and Tgfb1i1* mRNA under quiescent conditions were low but differed significantly among the three ES cell lines and that *fosB*$^{d/d}$ ES cells exhibited the highest levels of their expression. Thrombospondin 1 is known to activate the latent form of TGF-β1 through protein–protein interaction (Ren *et al.*, 2006). Therefore, TGF-β1 signaling is likely to be active in quiescent *fosB*$^{d/d}$ cells, and to a lesser extent in quiescent *fosB*-null ES cells as well, reflecting the expression levels of *Tgfb1* and *Thbs1* mRNAs.

Down-Regulation of Cell-Matrix Adhesion and TGF-β1 Signaling in fosB$^{FN/FN}$ *ES Cells*

To verify the role of FosB in cell-matrix adhesion and TGF-β1 signaling, we established *fosB*$^{FN/FN}$ ES cells in which FosB protein is exclusively translated from *fosB*^{F} mRNA (Figure 7A). Mutations introduced at alternative splicing donor and acceptor sites to avoid alternative splicing were confirmed by genomic sequencing (Supplementary Figure S4A). The exclusive expression of the longer *fosB*^{F} mRNA in exponentially growing *fosB*$^{FN/FN}$ cells was confirmed by RT-PCR, and its level was equivalent to those of *fosB* or Δ*fosB*

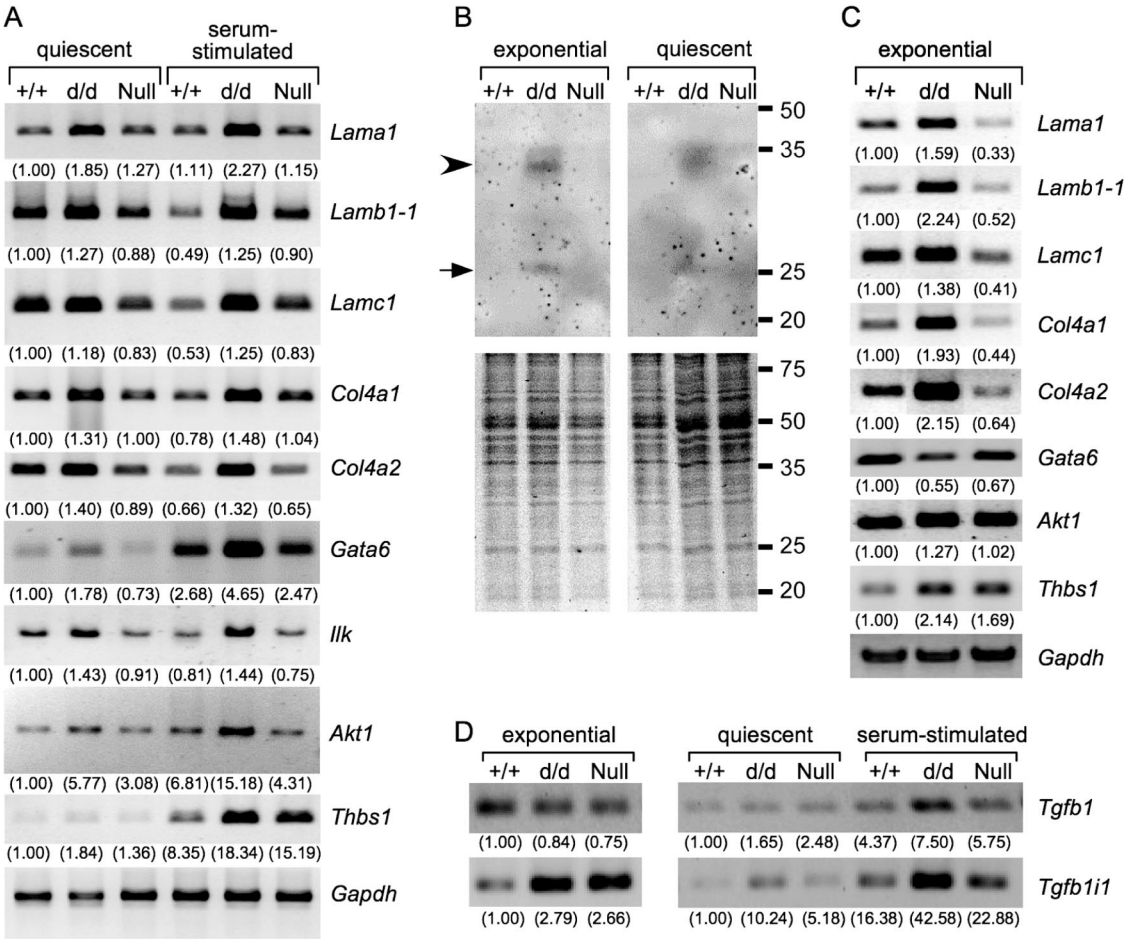

Figure 5. Altered gene expression profiles among *fosB* mutant and wild-type ES cells. (A) Expression of genes for basement membrane proteins. RNA prepared from quiescent ES cells or ES cells 4 h after serum stimulation were subjected to RT-PCR analysis. The relative amount of each RT-PCR product to that of the quiescent wild type was normalized with that of *Gapdh* mRNA and is shown in parentheses. (B) Expression of ΔFosB protein in $fosB^{d/d}$ ES cells. Nuclear extracts (200 μg per lane) prepared from exponentially growing or quiescent ES cells were subjected to Western blotting with anti-FosB(N; top panel). Membranes stained with CBB are shown (bottom panel). The arrowhead indicates p32/36, and the arrow indicates p24. (C). RT-PCR analysis of genes for basement membrane proteins in exponentially growing ES cells. The amount of each RT-PCR product relative to that of the wild type was normalized with that of *Gapdh* mRNA and is shown in parenthesis. (D) RT-PCR analysis of *Tgfb1* and *Tgfb1i1* expression. The amount of each RT-PCR product relative to that of the exponentially growing wild type (left panel, exponential) or to that of the quiescent wild type (right panel, quiescent and serum-stimulated) was normalized with that of *Gapdh* mRNA, and is shown in parentheses.

mRNAs in wild-type cells or to that of $fosB^{d}$ mRNA in $fosB^{dN/dN}$ cells (Figure 7B). In Western blotting analysis, the level of FosB protein in exponentially growing $fosB^{FN/FN}$ cells was again below the limit of detection (data not shown); however, we detected anti-FosB(C) immunoreactivity in exponentially growing $fosB^{FN/FN}$ and wild-type cells but not in $fosB^{d/d}$ cells (Supplementary Figure S4B), confirming that in exponential growth conditions, $fosB^{FN/FN}$ and wild-type cells do indeed express FosB protein.

We then analyzed expression levels of genes encoding basement membrane proteins as well as those involved in TGF-β1 signaling in exponentially growing cultures of various ES cell lines. Expression levels of *Lama1*, *Lamb1-1*, and *Col4a1, but not Lmac1, Col4a2* in $fosB^{FN/FN}$ ES cells were slightly lower than those in wild-type or *fosB*-null ES cells (data not shown). Among three genes involved in TGF-β1 signaling, only the level of *Tgfb1i1* expression was significantly reduced in $fosB^{FN/FN}$ ES cells, compared with those in wild-type ES cells, whereas a significant increase in *Tgfb1i1* expression in $fosB^{+/d}$, $fosB^{d/d}$ and *fosB*-null ES cells was again confirmed (Figure 7C). We thus concluded that FosB down-regulates expression of the *Tgfb1i1* gene, whereas ΔFosB/Δ2ΔFosB up-regulates its expression.

Because it was apparent that the $fosB^{d}$ allele expresses an increased level of the modified transcript, namely $fosB^{d}$ mRNA, compared with the wild-type ($fosB^{+}$) or to the modified allele with the *neo* cassette ($fosB^{dN}$; Figure 7B), we also analyzed the expression levels of genes encoding basement membrane proteins and those involved in TGF-β1 signaling in $fosB^{dN/dN}$ ES cells and found that expression levels of most of the genes examined were not significantly altered compared with levels in wild-type ES cells (data not shown), suggesting that the increased expression of these genes in $fosB^{d/d}$ ES cells is dependent on the increased level of ΔFosB/Δ2ΔFosB, but not on the loss of FosB expression.

We finally examined whether $fosB^{FN/FN}$ ES cells undergo any alteration in cell-matrix adhesion in comparison to other cell lines under exponential growth conditions (Figure 7D). Exponentially growing $fosB^{d/d}$ cells exhibited the highest adhesion to plates coated or not coated with gelatin or laminin,

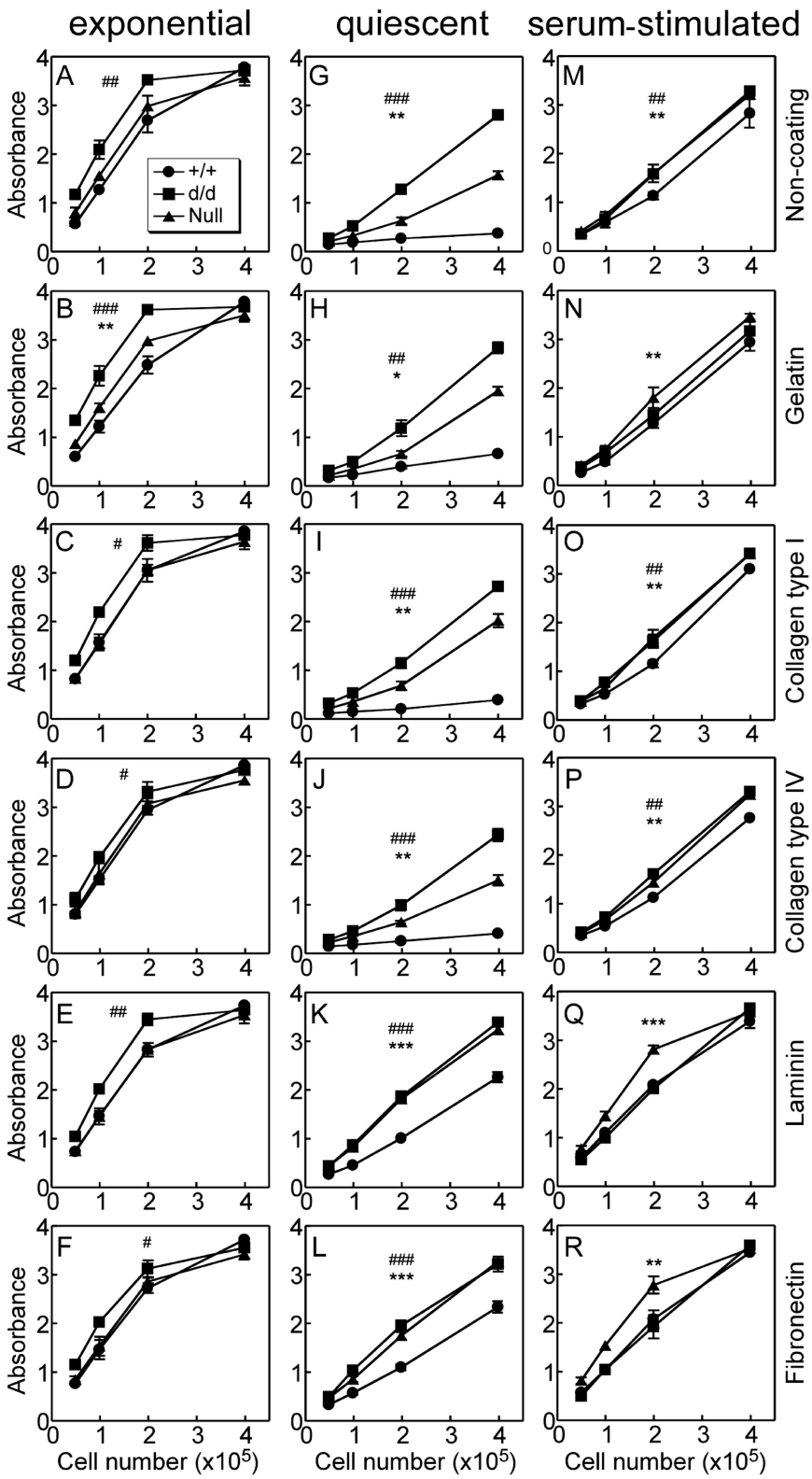

Figure 6. Increased cell-matrix adhesion in *fosB*$^{d/d}$ and *fosB*-null ES cells. Cell adhesion to five different matrices was examined using cells prepared under three different culture conditions: in an exponentially growing culture (A–F); a quiescent culture (G–L); and 4 h after serum stimulation (M–R), as described in *Materials and Methods.* The extent of cell adhesion is shown as the absorbance at 595 nm (mean ± SEM, n = 3). $^{\#}p < 0.05$; $^{\#\#}p < 0.01$; $^{\#\#\#}p < 0.001$; statistical difference between wild-type and *fosB*$^{d/d}$ ES cells. $^{*}p < 0.05$; $^{**}p < 0.01$, $^{***}p < 0.001$; statistical difference between wild-type and *fosB*-null ES cells.

compared with wild-type, *fosB*$^{+/d}$, *fosB*$^{dN/dN}$, *fosB*$^{FN/FN}$, and *fosB*-null ES cells. The *fosB*$^{FN/FN}$ cells exhibited the lowest adhesion to all matrices, especially to the uncoated and gelatin-coated plates, whereas *fosB*-null or *fosB*$^{+/d}$ ES cells again exhibited a slight increase in adhesion compared with wild-type ES cells (Figure 7D), indicating that FosB itself negatively regulates cell-matrix adhesion. The *fosB*$^{dN/dN}$ ES cells expressing the lower level of *fosB*^{d} mRNA equivalent to that of Δ*fosB* mRNA in wild-type cells exhibited essentially the same level of cell-matrix adhesion as that of wild-type ES cells.

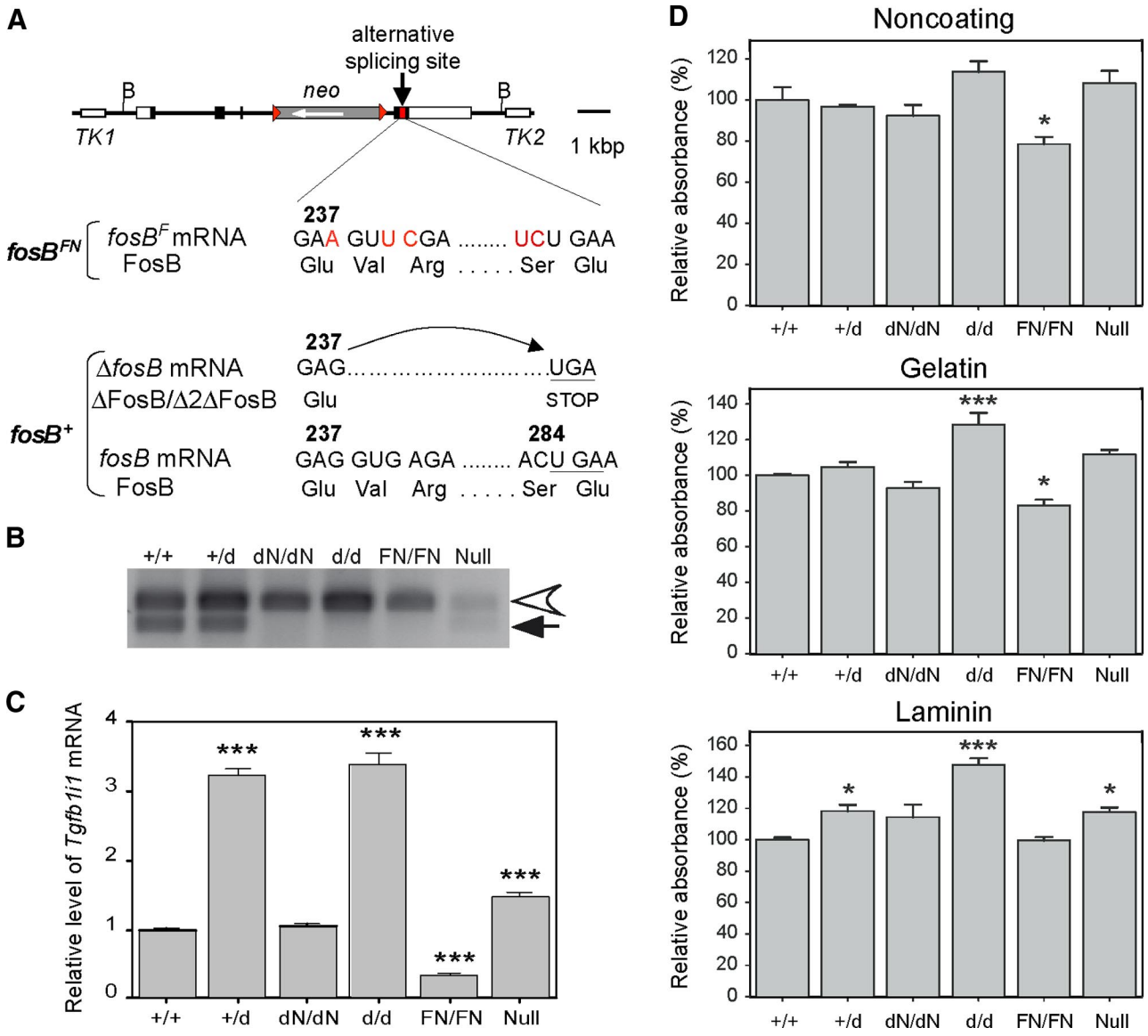

Figure 7. Decreased cell-matrix adhesion in *fosB*$^{FN/FN}$ ES cells. (A) Strategy for generation of a *fosB*^{FN} allele which encodes only FosB. The targeting vector, pTV*fosB*^{FN}, is flanked by two HSV-*TK* genes (*TK1, TK2*) at BamHI sites, labeled B. Five base substitutions (red letters) are introduced at the alternative splicing donor and acceptor sites in exon 4, and an inverted *neo* cassette (gray box) flanked by two *loxP* sites (red triangles) was placed in intron 3. Sequences of a transcript (*fosB*^{F} mRNA) from the *fosB*^{FN} allele or from the wild-type (*fosB*$^{+}$) allele, and corresponding amino acid residues are shown. The arc with the arrowhead indicates the alternative splicing of the exonic intron (red box). (B) RT-PCR analysis of *fosB* mRNAs in exponentially growing cells. *fosB* cDNA was amplified with primers FB7 and FB8. (C) Quantitative RT-PCR analysis of the *Tgfb1i1* gene in exponentially growing ES cells. The relative level of *Tgfb1i1* mRNA in each cell line to that of the wild type is shown as a bar graph (mean ± SEM, n = 3). (D) Cell-matrix adhesion was examined using exponentially growing cells at 2×10^5 cells per well. The extent of cell adhesion is shown as the absorbance (%) relative to absorbance at 595 nm for wild-type cells (mean ± SEM, n = 4). * $p < 0.05$; *** $p < 0.001$; statistical difference from wild-type cells using ANOVA.

DISCUSSION

In the present study, we created novel *fosB*^{d}, *fosB*^{dN}, and *fosB*^{FN} alleles. In the former two, termination codons were introduced into the *fosB* gene after the last codon for ΔFosB, whereas in the latter alternative splicing of an exonic intron in exon 4 was avoided by introducing five base substitutions at splicing donor and acceptor sites without amino acid substitution. We established ES cell lines that are homozygous for the *fosB*^{d}, *fosB*^{dN} and *fosB*^{FN} alleles after this knockin mutagenesis. These *fosB*$^{d/d}$ and *fosB*$^{dN/dN}$ homozygotes produce a modified *fosB*^{d} mRNA that encodes only ΔFosB and Δ2ΔFosB, whereas the *fosB*$^{FN/FN}$ homozygotes produce a modified *fosB*^{F} mRNA encoding only FosB. Interestingly, the *fosB*^{d} allele is likely to produce more *fosB*^{d} mRNA than is the *fosB*^{dN} allele, which produces an amount of transcript that is equivalent to that of the *fosB*$^{+}$ allele, resulting in greater production of its translation products. In cells with the *fosB*^{dN} allele, a *neo* cassette placed in the opposite direction may interfere with efficient transcription or processing of the *fosB*^{d} transcript. We confirmed that levels of ΔFosB and to a lesser extent Δ2ΔFosB proteins expressed in the *fosB*$^{d/d}$ homozygotes were significantly higher than the total amounts of FosB, ΔFosB, and Δ2ΔFosB proteins expressed in wild-type ES cells in any culture conditions examined. In addition

to the increased level of the *fosB*^{d} mRNA in *fosB*$^{d/d}$ cells, the higher stability of ΔFosB protein (Chen *et al.*, 1997) may account for this phenomenon. It is noteworthy that in serum-stimulated *fosB*$^{d/d}$ ES cells, the expression level of c-Fos but not Fra-1 and -2 proteins was apparently lower than in serum-stimulated wild-type and *fosB*-null cells (Figure 3E). It is most likely that the significantly higher levels of ΔFosB and Δ2ΔFosB proteins must cause depletion of free Jun proteins, which are also c-Fos protein partners; thus any liberated c-Fos, which is known to be a very unstable protein (Acquaviva *et al.*, 2001), may be rapidly degraded even in serum-stimulated cells.

To explore the impact of FosB or ΔFosB/Δ2ΔFosB on gene expression, we performed cDNA microarray analyses using RNA prepared from serum-stimulated wild-type, *fosB*$^{d/d}$, and *fosB*-null ES cells. We found that 203 genes were up-regulated and 19 were down-regulated in *fosB*$^{d/d}$ cells compared with *fosB*-null ES cells. However, compared with wild type, only 10 genes were up-regulated in both types of mutant ES cells, whereas three genes were down-regulated (Figure 4D). Because both mutant ES cells were devoid of FosB, genes whose expression was similarly altered in the two mutants are likely to be regulated by FosB. In contrast, genes whose expression was different between the two are considered to be regulated by ΔFosB/Δ2ΔFosB. These results are unexpected in that they imply that expression of a substantial number of genes is directly or indirectly regulated by ΔFosB and that expression of a much smaller number of genes is regulated by FosB, because FosB is a more potent transactivator than ΔFosB or Δ2ΔFosB (Nakabeppu and Nathans, 1991; Sabatakos *et al.*, 2008).

Reflecting the fact that more than a quarter of the genes up-regulated in *fosB*$^{d/d}$ ES cells encode cell-adhesion–related proteins (Table 2, Figure 5), cell-matrix adhesion of *fosB*$^{d/d}$ and to a lesser extent *fosB*-null ES cells was more efficient than that of the wild-type cells under the three respective culture conditions of exponential growth, quiescence, and serum stimulation. Cell-matrix adhesion of wild-type cells was the lowest at quiescence among the three conditions; however, *fosB*$^{d/d}$ or *fosB*-null cells exhibited significantly increased cell-matrix adhesion even in quiescence, compared with wild-type cells (Figure 6). Under conditions of exponential growth in the presence of serum or with serum stimulation of quiescent cells, all three cell lines exhibited significantly increased cell adhesion compared with that seen under serum-deprived quiescent conditions. As shown in Supplementary Figure S3, phosphorylation of Akt was also significantly increased in all three cell lines after serum stimulation. It is known that growth factors in serum activate Akt and that activated Akt induces expression of various cell-adhesion–related proteins and thus enhances cell adhesion (Li *et al.*, 2001; Lim *et al.*, 2003). Therefore, the absence of activated Akt in the quiescent wild-type cells may account for their having the lowest level of cell adhesion, whereas the increased expression of cell-adhesion–related proteins in the quiescent *fosB*$^{d/d}$ cells (Figure 5B), would contribute to the increased cell adhesion in the absence of Akt signaling.

Among the possible downstream targets of FosB or ΔFosB/Δ2ΔFosB, we focused on genes encoding proteins comprising the basement membrane and the TGF-β1 signaling pathway. The *fosB*$^{d/d}$ cells expressing only ΔFosB/Δ2ΔFosB exhibited a strongly increased expression of genes involved in the TGF-β1 signaling pathway including *Tgfb1i1* as well as genes encoding the basement membrane proteins, under the various culture conditions. In exponentially growing *fosB*$^{FN/FN}$ cells, which exclusively express FosB, we found that the expression level of the *Tgfb1i1* gene, but not those of genes encoding the basement membrane proteins, was the lowest among the wild-type, fosB$^{+/d}$, *fosB*$^{dN/dN}$, *fosB*$^{d/d}$, and *fosB*-null cell lines. Furthermore, we confirmed that *fosB*$^{FN/FN}$ cells exhibited the lowest cell-matrix adhesion among all cell lines under exponential growth conditions (Figure 7D). We thus conclude that ΔFosB and/or Δ2ΔFosB positively regulate cell-matrix adhesion as well as TGF-β1 signaling, whereas FosB negatively regulates them. Recently, it has been reported that Δ2ΔFosB and to a lesser extent ΔFosB modulate the expression and phosphorylation of Smads independent of intrinsic AP-1 activity (Sabatakos *et al.*, 2008), confirming that both ΔFosB and Δ2ΔFosB play important roles in the up-regulation of TGF-β1 signaling, as we observed in the present study.

TGF-β1 is known to stimulate the DNA-binding activity of AP-1 complex containing FosB or ΔFosB (Lai and Cheng, 2002). Furthermore, TGF-β1 stimulates gene expression through the cooperation of Smad3/Smad4 and AP-1 as a complex (Liberati *et al.*, 1999; Liang *et al.*, 2002). In *fosB*$^{d/d}$ ES cells, a gene for the Smad4-interacting transcription cofactor, *Cited1* (Plisov *et al.*, 2005), was also up-regulated (Table 3), suggesting that ΔFosB is involved in various steps of the TGF-β1 signaling pathway. Moreover, ΔFosB is likely to regulate gene expression through modulating mRNA stability as well as by modulating transcription itself (Nakabeppu and Nathans, 1991; Nakabeppu *et al.*, 1993; Oda *et al.*, 1995;

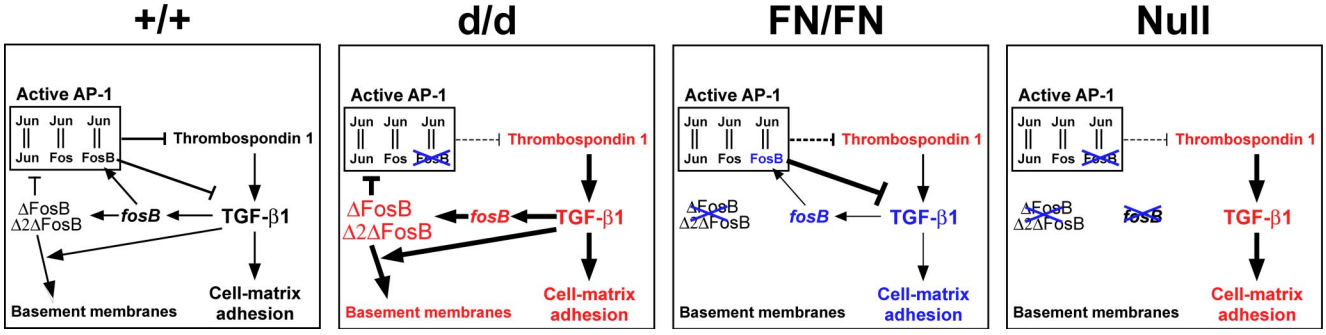

Figure 8. Signaling pathway for proceeding from FosB or ΔFosB/Δ2ΔFosB toward thrombospondin 1/TGF-β1, which regulates cell-matrix adhesion. Thrombospondin 1/TGF-β1 signaling, which may be negatively regulated by Jun/Fos complexes (active AP-1), enhances cell-matrix adhesion and up-regulates genes for basement membrane proteins through *fosB* gene expression. ΔFosB and Δ2ΔFosB antagonize not only FosB but also other Fos family members (Fos) constituting the major AP-1 complexes with the three Jun proteins (Jun), and they may up-regulate the TGF-β1 signaling pathway independent of intrinsic AP-1 activity. See details in the text and Supplemental Figure S2. Red represents up-regulated genes and blue indicates down-regulated genes.

Miura *et al.*, 2005). *Thbs1* encoding Thrombospondin 1 is known to activate latent TGF-β1 (Ren *et al.*, 2006). It has been reported that transcription of the *Thbs1* gene is suppressed by overexpression of c-Jun (Dejong *et al.*, 1999) and that FosB facilitates c-Jun function, whereas ΔFosB suppresses it by forming a heterodimer with c-Jun (Nakabeppu and Nathans, 1991). It is likely that FosB in wild-type ES cells down-regulates *Thbs1* expression together with c-Jun, thereby negatively regulating cell-matrix adhesion. In contrast, ΔFosB or Δ2ΔFosB represses the c-Jun function and thus may abrogate negative regulation of *Thbs1* expression by c-Jun resulting in the promotion of cell-matrix adhesion (Figure 8).

It has been reported that activin type II receptor (ACVR2), a member of the TGF-β type II receptor family, up-regulates expression of genes for AP-1 components, namely, *junD*, *c-jun*, and *fosB* (Deacu *et al.*, 2004). As upstream regulators of TGF-β1 signaling, KLF6, which transactivates genes for TGF-β1 signaling components (Botella *et al.*, 2002), and ELF3, which stimulates type II TGF-β receptor promoter (Kopp *et al.*, 2004), were up-regulated in $fosB^{d/d}$ ES cells (Table 3). Several downstream targets of TGF-β1 were also up-regulated in $fosB^{d/d}$ cells (Table 3), such as genes for RUNX1 (*Runx1*), a transcription factor known to induce a gene for a tissue inhibitor of metalloproteinase 1 (Bertrand-Philippe *et al.*, 2004), cardiac ankyrin repeat protein (*Ankrd1*) related to the initiation and regulation of arteriogenesis (Boengler *et al.*, 2003), and E-cadherin (*cdh1*), whose induction by TGF-β1 is mediated through the activation of focal adhesion kinase due to extracellular matrix remodeling and increased cell-matrix interactions (Wang *et al.*, 2004). It is suggested that both the expression and function of ΔFosB can be up-regulated downstream of the TGF-β1 signaling pathway and that these two features are in turn up-regulated as a result of antagonistic regulation by ΔFosB of Jun/Fos functioning as active AP-1, thereby generating a positive feedback circuit (Figure 8). Increased expression of ΔFosB in $fosB^{d/d}$ or $fosB^{+/d}$ ES cells but not in $fosB^{dN/dN}$ ES cells was observed even in quiescence, and this was most likely the result of such positive feedback. In $fosB^{FN/FN}$ cells, lack of the antagonistic action of ΔFosB on the active AP-1 complexes may further increase the negative regulation by FosB of the TGF-β1 signaling pathway. However, the complete lack of the *fosB* gene in *fosB*-null ES cells disallows these positive and negative feedbacks, resulting in the limited activation of Thrombospondin 1/TGF-β1 signaling in these cells (Figures 5D and 8).

The *Tgfb1i1* gene, also known as *Hic5/ARA55*, encodes a LIM-only member of the paxillin superfamily that serves as a component of focal adhesions as well as a steroid receptor coactivator (Yang *et al.*, 2000; Nishiya *et al.*, 2001), indicating that the stronger expression of *Tgfb1i1* may account in part for the higher level of cell-matrix adhesion. It has been shown that expression of the *Tgfb1i1* gene is regulated by RAR as well as by TGF-β1, both of which can modulate AP-1 function (Liberati *et al.*, 1999; Zhou *et al.*, 1999; Suzukawa and Colburn, 2002; Zhuang *et al.*, 2003), suggesting that expression of *Tgfb1i1* is indirectly regulated by FosB or ΔFosB/Δ2ΔFosB through their interaction with steroid receptors or Smad proteins, as reported recently (Sabatakos *et al.*, 2008). Furthermore, it has been shown that Hic5/ARA55 itself negatively regulates Smad3 signaling (Wang *et al.*, 2005). At the present time, we cannot explain why the expression level of the *Tgfb1i1* gene in *fosB*-null cells is as high as in $fosB^{+/d}$ or $fosB^{d/d}$ cells that express increased levels of ΔFosB, although it does appear that ΔFosB positively regulates the expression of the *Tgfb1i1* gene in a dose-dependent manner (Figure 7C). Availability of various cell lines that express different levels of either FosB or ΔFosB/Δ2ΔFosB would help to shed light on the complex regulation of gene expression and cell-matrix adhesion. Furthermore, the establishment of cell lines that exclusively express ΔFosB or Δ2ΔFosB with or without FosB is also greatly important.

ACKNOWLEDGMENTS

We thank Dr. M. Katsuki (National Institutes of Natural Sciences, Tokyo, Japan) for CCE ES cells, M. Otsu in the Laboratory for Technical Support, Medical Institute of Bioregulation for the DNA sequence analyses, A. Matsuyama for animal care, and Dr. W. Campbell for comments on the manuscript. We also thank all members of our laboratory for their helpful discussions. This work was supported by grants from CREST, Japan Science and Technology Agency, the Ministry of Education, Culture, Sports, Science, and Technology of Japan (Grant number: 16012248), and the Japan Society for the Promotion of Science (Grants 16390119 and 18300124).

REFERENCES

Acquaviva, C., Ferrara, P., Bossis, G., Brockly, F., Salvat, C., Jariel-Encontre, I., and Piechaczyk, M. (2001). Degradation of cellular and viral Fos proteins. Biochimie *83*, 357–362.

Bertrand-Philippe, M., Ruddell, R. G., Arthur, M. J., Thomas, J., Mungalsingh, N., and Mann, D. A. (2004). Regulation of tissue inhibitor of metalloproteinase 1 gene transcription by RUNX1 and RUNX2. J. Biol. Chem. *279*, 24530–24539.

Boengler, K., Pipp, F., Fernandez, B., Ziegelhoeffer, T., Schaper, W., and Deindl, E. (2003). Arteriogenesis is associated with an induction of the cardiac ankyrin repeat protein (carp). Cardiovasc. Res. *59*, 573–581.

Botella, L. M. *et al.* (2002). Transcriptional activation of endoglin and transforming growth factor-β signaling components by cooperative interaction between Sp1 and KLF6, their potential role in the response to vascular injury. Blood *100*, 4001–4010.

Chen, J., Kelz, M. B., Hope, B. T., Nakabeppu, Y., and Nestler, E. J. (1997). Chronic Fos-related antigens: stable variants of ΔFosB induced in brain by chronic treatments. J. Neurosci. *17*, 4933–4941.

Deacu, E. *et al.* (2004). Activin type II receptor restoration in ACVR2-deficient colon cancer cells induces transforming growth factor-β response pathway genes. Cancer Res. *64*, 7690–7696.

Dejong, V., Degeorges, A., Filleur, S., Ait-Si-Ali, S., Mettouchi, A., Bornstein, P., Binetruy, B., and Cabon, F. (1999). The Wilms' tumor gene product represses the transcription of thrombospondin 1 in response to overexpression of c-Jun. Oncogene *18*, 3143–3151.

Ekblom, P., Lonai, P., and Talts, J. F. (2003). Expression and biological role of laminin-1. Matrix Biol. *22*, 35–47.

Ide, Y., Tsuchimoto, D., Tominaga, Y., Iwamoto, Y., and Nakabeppu, Y. (2003). Characterization of the genomic structure and expression of the mouse Apex2 gene. Genomics *81*, 47–57.

Kopp, J. L., Wilder, P. J., Desler, M., Kim, J. H., Hou, J., Nowling, T., and Rizzino, A. (2004). Unique and selective effects of five Ets family members, Elf3, Ets1, Ets2, PEA3, and PU1, on the promoter of the type II transforming growth factor-β receptor gene. J. Biol. Chem. *279*, 19407–19420.

Kurushima, H. *et al.* (2005). Selective induction of ΔFosB in the brain after transient forebrain ischemia accompanied by an increased expression of galectin-1, and the implication of ΔFosB and galectin-1 in neuroprotection and neurogenesis. Cell Death Differ. *12*, 1078–1096.

Lai, C. F., and Cheng, S. L. (2002). Signal transductions induced by bone morphogenetic protein-2 and transforming growth factor-beta in normal human osteoblastic cells. J. Biol. Chem. *277*, 15514–15522.

Lawler, J. (2002). Thrombospondin-1 as an endogenous inhibitor of angiogenesis and tumor growth. J. Cell. Mol. Med. *6*, 1–12.

Lazo, P. S., Dorfman, K., Noguchi, T., Mattei, M. G., and Bravo, R. (1992). Structure and mapping of the *fosB* gene. FosB downregulates the activity of the *fosB* promoter. Nucleic Acids Res. *20*, 343–350.

Li, L., Arman, E., Ekblom, P., Edgar, D., Murray, P., and Lonai, P. (2004). Distinct GATA6- and laminin-dependent mechanisms regulate endodermal and ectodermal embryonic stem cell fates. Development *131*, 5277–5286.

Li, X., Talts, U., Talts, J. F., Arman, E., Ekblom, P., and Lonai, P. (2001). Akt/PKB regulates laminin and collagen IV isotypes of the basement membrane. Proc. Natl. Acad. Sci. USA *98*, 14416–14421.

Liang, C. L., Chen, J. L., Hsu, Y. P., Ou, J. T., and Chang, Y. S. (2002). Epstein-Barr virus BZLF1 gene is activated by transforming growth factor-β

through cooperativity of Smads and c-Jun/c-Fos proteins. J. Biol. Chem. *277*, 23345–23357.

Liberati, N. T., Datto, M. B., Frederick, J. P., Shen, X., Wong, C., Rougier-Chapman, E. M., and Wang, X. F. (1999). Smads bind directly to the Jun family of AP-1 transcription factors. Proc. Natl. Acad. Sci. USA *96*, 4844–4849.

Lim, I. J., Phan, T. T., Tan, E. K., Nguyen, T. T., Tran, E., Longaker, M. T., Song, C., Lee, S. T., and Huynh, H. T. (2003). Synchronous activation of ERK and phosphatidylinositol 3-kinase pathways is required for collagen and extracellular matrix production in keloids. J. Biol. Chem. *278*, 40851–40858.

McClung, C. A., Ulery, P. G., Perrotti, L. I., Zachariou, V., Berton, O., and Nestler, E. J. (2004). DFosB: a molecular switch for long-term adaptation in the brain. Brain Res. Mol. Brain Res. *132*, 146–154.

Miura, T., Ohnishi, Y., Kurushima, H., Horie, H., Kadoya, T., and Nakabeppu, Y. (2005). Regulation of the neuronal fate by ΔFosB and its downstream target, galectin-1. Curr. Drug Targets *6*, 437–444.

Nakabeppu, Y., and Nathans, D. (1991). A naturally occurring truncated form of FosB that inhibits Fos/Jun transcriptional activity. Cell *64*, 751–759.

Nakabeppu, Y., Oda, S., and Sekiguchi, M. (1993). Proliferative activation of quiescent Rat-1A cells by ΔFosB. Mol. Cell. Biol. *13*, 4157–4166.

Nakabeppu, Y., Ryder, K., and Nathans, D. (1988). DNA binding activities of three murine Jun proteins: stimulation by Fos. Cell *55*, 907–915.

Nishioka, T., Sakumi, K., Miura, T., Tahara, K., Horie, H., Kadoya, T., and Nakabeppu, Y. (2002). *fosB* gene products trigger cell proliferation and morphological alteration with an increased expression of a novel processed form of galectin-1 in the rat 3Y1 embryo cell line. J. Biochem. *131*, 653–661.

Nishiya, N., Tachibana, K., Shibanuma, M., Mashimo, J. I., and Nose, K. (2001). Hic-5-reduced cell spreading on fibronectin: competitive effects between paxillin and Hic-5 through interaction with focal adhesion kinase. Mol. Cell. Biol. *21*, 5332–5345.

Oda, S., Nishida, J., Nakabeppu, Y., and Sekiguchi, M. (1995). Stabilization of cyclin E and cdk2 mRNAs at G1/S transition in Rat-1A cells emerging from the G0 state. Oncogene *10*, 1343–1351.

Plisov, S., Tsang, M., Shi, G., Boyle, S., Yoshino, K., Dunwoodie, S. L., Dawid, I. B., Shioda, T., Perantoni, A. O., and de Caestecker, M. P. (2005). Cited1 is a bifunctional transcriptional cofactor that regulates early nephronic patterning. J. Am. Soc. Nephrol. *16*, 1632–1644.

Rancourt, D. E., Tsuzuki, T., and Capecchi, M. R. (1995). Genetic interaction between hoxb-5 and hoxb-6 is revealed by nonallelic noncomplementation. Genes Dev. *9*, 108–122.

Ren, B., Yee, K. O., Lawler, J., and Khosravi-Far, R. (2006). Regulation of tumor angiogenesis by thrombospondin-1. Biochim. Biophys. Acta *1765*, 178–188.

Robertson, E. J. (1987). Tetracarcinomas and Embryonic Stem Cells: A Practical Approach, New York: IRL Press.

Sabatakos, G. *et al.* (2000). Overexpression of ΔFosB transcription factor(s) increases bone formation and inhibits adipogenesis. Nat. Med. *6*, 985–990.

Sabatakos, G., Rowe, G. C., Kveiborg, M., Wu, M., Neff, L., Chiusaroli, R., Philbrick, W. M., and Baron, R. (2008). Doubly truncated FosB isoform (Δ2ΔFosB) induces osteosclerosis in transgenic mice and modulates expression and phosphorylation of Smads in osteoblasts independent of intrinsic AP-1 activity. J. Bone Miner. Res *23*, 584–595.

Sarkar, G., and Sommer, S. S. (1990). The "megaprimer" method of site-directed mutagenesis. Biotechniques *8*, 404–407.

Shaulian, E., and Karin, M. (2001). AP-1 in cell proliferation and survival. Oncogene *20*, 2390–2400.

Suzukawa, K., and Colburn, N. H. (2002). AP-1 transrepressing retinoic acid does not deplete coactivators or AP-1 monomers but may target specific Jun or Fos containing dimers. Oncogene *21*, 2181–2190.

Tahara, K., Tsuchimoto, D., Tominaga, Y., Asoh, S., Ohta, S., Kitagawa, M., Horie, H., Kadoya, T., and Nakabeppu, Y. (2003). ΔFosB but not FosB induces delayed apoptosis independent of cell proliferation in the Rat1a embryo cell line. Cell Death Differ. *10*, 496–507.

Tsuchimoto, D., Sakai, Y., Sakumi, K., Nishioka, K., Sasaki, M., Fujiwara, T., and Nakabeppu, Y. (2001). Human APE2 protein is mostly localized in the nuclei and to some extent in the mitochondria, while nuclear APE2 is partly associated with proliferating cell nuclear antigen. Nucleic Acids Res. *29*, 2349–2360.

Wang, H., Radjendirane, V., Wary, K. K., and Chakrabarty, S. (2004). Transforming growth factor β regulates cell-cell adhesion through extracellular matrix remodeling and activation of focal adhesion kinase in human colon carcinoma Moser cells. Oncogene *23*, 5558–5561.

Wang, H., Song, K., Sponseller, T. L., and Danielpour, D. (2005). Novel function of androgen receptor-associated protein 55/Hic-5 as a negative regulator of Smad3 signaling. J. Biol. Chem. *280*, 5154–5162.

Xu, P., Yoshioka, K., Yoshimura, D., Tominaga, Y., Nishioka, T., Ito, M., and Nakabeppu, Y. (2003). In vitro development of mouse embryonic stem cells lacking JSAP1 scaffold protein revealed its requirement during early embryonic neurogenesis. J. Biol. Chem. *278*, 48422–48433.

Yang, L., Guerrero, J., Hong, H., DeFranco, D. B., and Stallcup, M. R. (2000). Interaction of the tau2 transcriptional activation domain of glucocorticoid receptor with a novel steroid receptor coactivator, Hic-5, which localizes to both focal adhesions and the nuclear matrix. Mol. Biol. Cell *11*, 2007–2018.

Zhou, X. F., Shen, X. Q., and Shemshedini, L. (1999). Ligand-activated retinoic acid receptor inhibits AP-1 transactivation by disrupting c-Jun/c-Fos dimerization. Mol. Endocrinol. *13*, 276–285.

Zhuang, Y., Faria, T. N., Chambon, P., and Gudas, L. J. (2003). Identification and characterization of retinoic acid receptor β2 target genes in F9 teratocarcinoma cells. Mol. Cancer Res. *1*, 619–630.